Evidences of wider latewood in *Pinus sylvestris* from a forest-steppe of Southern Siberia

Alberto Arzac [a], Elena. A. Babushkina [b], Patrick Fonti [c], Viktoriya Slobodchikova [a], Irina V. Sviderskaya [a] & Eugene A. Vaganov [a,d]

[a] Siberian Federal University, 79 Svobodny pr., 660041 Krasnoyarsk, Russia

[b] Khakas Technical Institute, Branch of Siberian Federal University, 27 Shchetinkina St., 655017, Abakan, Russia

[c] Swiss Federal Institute for Forest, Snow and Landscape Research WSL, Zuercherstrasse 111, CH-8903 Birmensdorf, Switzerland

[d] V. N. Sukachev Institute of Forest, Siberian Branch of the Russian Academy of Sciences, Akademgorodok 50/28, Krasnoyarsk, Russia 660036

Corresponding author: Alberto Arzac, aarzak@sfu-kras.ru +7 (902) 979 96 95

Abstract

Climate affects wood formation with consequences for the functioning and survival of trees. Since tree-rings tissues (i.e., earlywood and latewood) are formed at different time in the season, the impact of climate change might differently affect their functions.

In this study, we combine quantitative tracheid anatomy with the Vaganov-Shashkin growth model (VS-model) to investigate how summer drought affected the annual ring structure of *Pinus sylvestris* L. from a forest-steppe zone in Southern Siberia. In particular, we used climate-growth relationships over a 50-year period to identify the timing of climatic signal of early-, transition-, and late-wood tracheid's diameters (D_{EW}, D_{TW} and D_{LW}). Corresponding daily growth rates (Gr) obtained by the VS-model were applied to calculate the changes in the width of the relative tree-ring sectors considering different levels of aridity.

Results indicate that tracheid size is sensitive to drought with temporal shifts among the climatic signal of D_{EW} (in May), D_{TW} (June) and D_{LW} (July). A comparison of modeled daily-growth rate cumulated over the climatic window of each ring sector and grouped by years with different level of aridity, indicated that a release of summer drought mostly affected the widths of the transition (+ 28.1%) and (+ 48.6%) latewood sectors, thus matching observations performed on the same cores.

These results suggest that current changes in climate seasonality, as occurring in the selected area, are positively impacting both the hydraulic efficiency (by increasing the diameter of the earlywood cells) and the latewood width of the wood produced in the area.

Keywords: climate change, drought, tracheidogram, VS-oscilloscope, xylem anatomy.

Introduction

While growing, trees fix a significant fraction of atmospheric carbon into their wood (Dixon et al., 1994; Lal, 2008), providing an important service in regulating the global carbon cycle. However, trees development is severely affected by climate conditions, which in turn affects their growth and survival with major consequences to their contribution as "carbon sinker" (Frank et al., 2015; Zhao and Running, 2010) and on the functioning of forest ecosystems. So for example, when facing drought, trees reduce transpiration to protect their tissues from extensive water loss and avoid hydraulic failures (Irvine et al., 1998). These physiological responses however affect the capacity to photo-assimilate atmospheric carbon and the turgor pressure of the growing cell which modify the amount, the structure (Fonti et al., 2010; Steppe et al., 2015), and the functioning (e.g., hydraulic efficiency and safety, mechanical support and storage of water and reserves) of the forming tree ring, representing an important legacy for future tree performance (e.g., biomass production and resilience capacity; Anderegg et al., 2015; Hereş *et al.*, 2014).

Tree-ring formation and structure results from a complex process of consecutive forming cells undergoing different phases of development (Rathgeber et al., 2016) which are continuously modulated by external and internal factors (Dengler, 2001; Hsiao and Acevedo, 1974; Růžička et al., 2015). The resulting tree-ring width and structure are highly dependent on the timing and magnitude of the climatic factor occurring during or prior the cell developmental phases as cell division, expansion and wall thickening (e.g., Castagneri *et al.*, 2017; Björklund et al., 2017; Rathgeber, 2017) . Xylem cells traits as cell size, wall thickness and wall to lumen ratio thus can reflect different detailed seasonal information depending on their position in the ring (Cuny et al., 2014; Olano et al., 2012) and be used to identify the main factors controlling tree

68 growth or to reconstruct past climatic conditions (Eckstein, 2004; Fonti and Jansen,
69 2012; Vaganov, 1990).
70 However, ongoing climate change may have diverse impacts on the different tree-ring
71 sectors (and functions) depending on the seasonality of its changes (e.g., Oladi *et al.*,
72 0217). Conifer tree-rings have a universal structure characterized by large thin-walled
73 tracheid formed at the beginning of the growing season (in the earlywood) which
74 progressively become smaller and thicker in the second part of the season (in the
75 latewood). Since this different cell structure serves diverse functions - more oriented
76 toward an efficient sap transport in the earlywood and toward mechanical stability in the
77 latewood - an alteration of the climate seasonality might engenders an unbalance of the
78 xylem functions.
79 Understanding which climatic factor affects which tree-ring sector is thus important to
80 assess the impact of changing climatic seasonality on the tree-ring structure and
81 functioning. Easy methods to assess these impacts are however still missing. Although
82 monitoring cambial activity is an important way to provide crucial information about
83 how the environment controls intra-annual tree growth (e.g., Camarero *et al.*, 2010;
84 Cocozza *et al.*, 2016; Rossi et al., 2006), long-term studies (with more than 5-10 years
85 of observations) are usually lacking. Similarly, quantitative wood anatomy can
86 retrospectively provide impact on the cell structure (Carrer et al., 2017; Castagneri et
87 al., 2017), however these studies are still time-consuming and usually limited in time
88 and space (Fonti et al., 2010) and miss to quantify the impacts on number of cells per
89 sector (sector width).
90 Process-based growth models are an efficient tool to understand and up-scale tree
91 growth response to several environmental conditions (Sass-Klaassen et al., 2016).
92 Specifically, the Vaganov-Shashkin model (VS-model, Vaganov *et al.*, 2006), due to its

design that allow to calculate daily tree-ring growth rates under given daily climatic conditions as temperature and soil moisture (see Anchukaitis *et al.*, 2006; Evans *et al.*, 2006; Vaganov *et al.*, 2006 for a model description and application), might be of additional help to assess the impact of changing climatic seasonality on the different ring sectors.

In this work, we combine climatic signal encoded into the wood cells with VS-model output on growth rates to infer how changes in seasonality affect the intra-annual tree-ring growth, with specific focus on the different tree-ring sectors (EW = earlywood, TW = transition wood, and LW = latewood) and their anatomical properties. Specifically, we focused on a widely studied species (i.e.; *Pinus sylvestris* L.) that inhabits a wide diversity of environments from southern Spain to northeast Asia (Nikolov and Helmisaari, 1992), and which is growing in a dry continental forest-steppe zone in Southern Siberia currently characterized by increasing summer precipitations (Anisimov et al., 2008). In particular we aimed at (*i*) collecting and using tree-ring width data from 20 trees over the period 1940 to 2013 to calibrate the VS-model to the selected site and species; (ii) collecting cell anatomical data for a subsample of 5 trees over the period 1964 to 2013 to build tracheidogram to identify the time of climatic sensitivity of the tracheid diameter in each ring sector (EW, TW and LW); and (iii) applying the model to assess how cumulated daily growth over these timing is differently affecting the ring width of these tree-ring sectors under changing level of summer drought. These last results have then been compared with measurements of the sectors width to validate model output with observations.

Materials and Methods

Study area

The study has been performed on wood material collected from a forest-steppe zone in Southern Siberia near the village of Malaya Minusa (Krasnoyarsk Krai, Russia, 53°43'N, 91°47'E, 300 m asl; Fig. 1A). According to the climatic data from the Minusinsk weather station (at 25 km from sampling site, 53°70'N, 91°70'E, 254 m asl, period 1935-2013), the area is characterized by dry continental climate conditions, with a mean annual temperature of 1.1 °C and annual precipitation of 328 mm (Fig. 1B). Precipitation mainly occurs in summer with a maximum in July, while mean daily temperature above 5 °C are from April to October and first early frosts usually happen in November. A trend analysis of the climatic data has revealed that during the period 1935-2013 the mean annual temperature and precipitation have increased at a rate of 0.31 ºC and 14.25 mm per decade, mainly caused by winter (December to February) warming and by an increased summer (June to August) wetting.

The vegetation at the sampling site is mainly composed by an open mixed forest stand of *P. sylvestris* and *Betula pendula* (Roth) growing within a matrix of shrubs and grasses (e.g., *Cotoneaster melanocarpus* (Bunge) Loudon, *Caragana arborescens* Lam., *Spiraea chamaedryfolia* L.; Babushkina *et al.*, 2015). The soils are sandy and covered by a humus layer of 10-15 cm (*Agroclimatic Resources of Krasnoyarsk Krai and Tuva*, 1974).

Wood sampling and tree-ring dating

Twenty dominant or codominant *P. sylvestris* trees were sampled in August 2014. Two 5-mm diameter wood cores were taken at stem breast height of each tree using a Pressler increment borer. Cores were labeled and taken to the laboratory where they were air-dried, glued to wood supports and manually polished with progressively finer sandpaper until the xylem cellular structure was clearly visible under magnification.

After visual cross-dating, tree-ring width (**RW**) were measured to the nearest 0.001 mm by using a LINTAB-5 sliding stage micrometer interfaced with the specialized software TSAP Win (RINNTECH, Heidelberg, Germany). Cross-dating accuracy was checked using the software COFECHA (Grissino-Mayer, 2001).

Measuring anatomical features

Xylem anatomical traits were measured on micro-sections from a subsample of five trees (one core per tree, average correlation to the mean chronology r = 0.86) for a period of 50 years (1964 to 2013). Permanent histological preparations were processed according to (Schweingruber and Poschlod, 2005). Cross-sections thinner than 20 µm were cut with a sledge microtome (Microm HM 430, Thermo Fisher Scientific, USA) and stained with Alcian blue (1% solution in acetic acid) and safranin (1% solution in ethanol) to distinguish unlignified cells (blue) and lignified cells (red).

Thin-sections were dehydrated using solutions with increasing ethanol concentrations, washed with xylol, and permanently preserved into Canada balsam. Images were captured with a digital camera (AXIOCam MRc5, Zeiss Germany) mounted on an optical microscope (Axio Imager D1, Zeiss, Germany) with a 200x magnification (see Fig. 2). Tracheid anatomical measurements – specifically the tracheid lumen diameter (**LRD**), the tracheid wall thickness (**CWT**) and the derived tracheids radial diameter (**D** = LRD+2CWT) – were performed along the radial axis of five radial files per ring using the Lineyka 2.01 software (Silkin, 2010, see also Fig. S.1).

Cell measurements along the radial file of the same ring have been first normalized to the mean number of cells and averaged to obtain a tracheidogram of the ring (Vaganov, 1990) using the ProcessorKR software (Silkin, 2010). The tracheidograms of D and CWT have been used to determine the radial cell diameter of the largest earlywood

tracheid (**D_{EW}**), the largest tracheid in the transition wood (**D_{TW}**), and of the tracheid displaying the largest cell wall thickness in the latewood (**D_{LW}**) (Table 1, Fig. 2).

Climate-growth relationship

Climate-growth relationships were performed to identify the climatic signal encoded into the tree-ring width (RW) and the diameter of the tracheid of the three zones within the ring (D_{EW}, D_{TW}, D_{LW}). Individual tree-ring time series were detrended using a 32-years spline function with a 50% frequency using the ARSTAN software (Cook and Holmes, 1996) to remove low-medium frequency information (Cook and Peters, 1981). Xylem traits chronologies (RW, D_{EW}, D_{TW}, D_{LW}) were finally obtained by averaging the time-series.

The climatic signals have been assessed by calculating Pearson's correlations between the chronologies of the selected tree-ring traits and the temperature (**T**), precipitation (**P**), and standardized precipitation-evapotranspiration index (**SPEI**, time-scale of 1 months; Vicente-Serrano *et al.*, 2010).The correlations have been performed using daily climatic data from the weather station of Minusinsk for the 50-years period (1964-2013) corresponding to the xylem anatomical measurements, with both a monthly resolution (from previous year September to September of the current year) and additionally with an 11-days moving window to ensure that climatic signal of fast forming tracheids (e.g. earlywood cells) is captured. Additionally, to assess the stability of the climatic signal over time for the most relevant months were re-assessed by separating two 25-year periods, i.e., for the early time (1964-1988) and for the more recent time (1989-2013).

Modeling daily tree-growth and estimating intra-ring widths

192 The Vaganov-Shashkin model (Vaganov et al., 2006) has been used to estimate the
193 daily growth rates (**Gr**) for each day over a 74-years period (1940-2013, extending the
194 period with xylem traits measurements to increase the number of years with modeled
195 growth rates). This model makes use of two pre-defined growth-limiting functions to
196 assess the achievable growth proportion given the temperature and soil moisture
197 conditions occurring at every day of the year. The daily tree-ring growth corresponds to
198 the Gr of the most limiting factor (temperature or soil moisture) weighted by the
199 available day length (photoperiod) for the given day at the site location. The sum of all
200 Gr of the year is thus a good estimate of the ring-width chronology index for that
201 specific year.
202 The VS-oscilloscope (Shishov et al., 2016) – a user friendly interface to interact with
203 the model – has been used to calibrate, verify and run the model. Model calibration and
204 verification have been performed by comparing the modeled annual ring-width
205 estimates with the detrended tree-ring chronology of the 20 sampled trees. Calibration
206 was performed for the years 1940-1989 and the verification on the subsequent years
207 1990-2013. Daily temperature and precipitation data from Minusinsk were used as
208 model input.
209 The timing of the significant ($P < 0.05$) response to precipitation along the moving
210 window of each intra-annual traits (D_{EW}, D_{TW} and D_{LW}) has been used to assign the Gr
211 relative to the intra-annual ring zone (i.e., the earlywood, latewood and transition wood)
212 and to estimates how drought releases affects their relative proportions. Daily Gr and
213 cumulative Gr for each tree-ring zone have then been calculated with the calibrated
214 model using the average daily temperature and precipitation data over the full period
215 (1940-2013). Additionally, we ranked the years from 1940 to 2013 according to their
216 growing season aridity index (based on the SPEI index values from May to September)

and grouped in three aridity groups. The 25 years with largest SPEI were assigned to the Wet group, the 25 years with lowest SPEI in the Dry group, and the 24 remaining years into the Medium aridity group. The variations in cumulative Gr have been estimated as absolute value and as percentage relative to the Dry group. For model validation, we calculated earlywood (**EW**) and latewood (**LW**) widths from the tracheidograms for the period 1964-2013, to analyze the variation in EW and LW widths in the three levels of aridity according to the SPEI index.

Results

Tree-ring chronologies and responses to climate

Ring width (RW) was analyzed in 20 trees aging between 77 and 115 years. The RW residual chronology showed a high common (inter-series correlation Rbt = 0.56, Expressed population signal EPS = 0.84) and sensitive (mean sensitivity MS = 0.29) signal. The first order autocorrelation was 0.29. Ring-width chronology was significantly correlated with the cell anatomical traits chronologies ($r = 0.4 – 0.67$; $P < 0.01$, see Table S.1).

Pearson's correlation revealed strong links between the tree-ring chronologies (RW, D_{EW}, D_{TW} and D_{LW}) and the climatic parameters (Table 2). These robust correlations indicate strong growth sensitivities to late spring and summer drought, when all the parameters showed both significant positive responses to precipitation and negative to temperature. A positive signal to precipitations also emerged for previous year November. Despite this strong general pattern, results also indicated a temporal shift of about two months in the timing of the climatic responses of the cell diameter while moving along the annual ring (Fig. 3). The signal of the largest earlywood tracheid (D_{EW}) mainly occurred between May and June (significant at $P < 0.05$ for DOY from

133 to 163) while for D_{LW} the response was mainly centered in July (DOY from 187 to 2011). These timings were almost not overlapping each other while the climatic signal of RW extended from DOY 127 to 196, thus extending over the timing of the climatic signal of the cell diameters. The maximal strength of the climatic signal was slightly reduced along the tree ring, i.e., changing from r = 0.52 on June 03rd for D_{EW}, to r = 0.47 on June 24th for D_{TW} in the transition wood, to r = 0.45 on July 21st for D_{LW} in the latewood.

The comparison of the signal between the two 25-years sub-period indicated a general decrease in the strength of the May-June climatic signal of the recent time (1989-2013) compared to the earlier time (1964-1988) (Table 3). An increase of signal strength of precipitation and SPEI in August (D_{TW}) was also observed.

Model simulations and impact of aridity on cumulative intra-ring growth rates

The correlation between calibration and verification periods of the VS-model with the indexed tree-ring chronology of the site was highly significant ($P < 0.001$, Fig. S.2; the calibrated model parameters applied are listed in the Table S.2). The correlation in the calibration period (1940–1988) was r = 0.57 with a Gleichläufigkeit (glk, i.e.; the coefficient of synchrony between two time series, see e.g.; Beck et al., (2013)) of 68.0 %, while for the verification period (1989–2013) the correlation was r = 0.66 with a glk of 83.3 %. For the full period (1940–2013) we obtained an r = 0.58 and 74.3 % glk. According to growth simulations performed for every year over the full available period (1940-2013), growing season length averaged 131 ± 11 days (mean ± SD), starting on May 17th (DOY 137 ± 9) and ending on September 26th (DOY 269 ± 7), with growth usually peaking on May 21st (DOY 141). Model simulation also indicated that growth is generally limited by temperature at the beginning and the end of the growing season

(from autumn to mid-spring) and by soil moisture from late spring (DOY 115) to late summer (DOY 228) (Fig. 4).

When comparing the timing of the significant precipitation signals from the cell diameters of the different ring sectors (D_{EW}, D_{TW} and D_{LW}) with the simulated growth rate curve (Gr), we observed that most of the growing season is not covered by their climatic signal (indicated as "Rest"; DOY 212 to 279; Fig. 4). The calculations of the cumulative growth rates grouped by years with different level of aridity (Fig. 5 and Table 4) indicated that a release of drought principally affected the width of the latewood. When comparing the sector widths between the Wet and the Dry group, we obtained a relative change of cumulated Gr of 8.5%, 28.1%, and 48.6 % over the timing of the significant climatic signal of D_{EW}, D_{TW} and D_{LW}, respectively. It has to be noted that model simulations also indicated a large increases (+40.4%) of the cumulative Gr for the part of the growing season not covered by climatic signal (Rest). These model results comparison between the sector widths of the dry and wet group matched well with EW and LW widths derived by the tracheidogram, whereby EW and LW has been observed to increase by 21.5% and 41.3%, respectively (Table 4).

Discussion

The combination of quantitative wood anatomy with the VS-growth modeling allowed us to disclose the influence of climate on the intra-annual tree-ring traits of *Pinus sylvestris* growing in a drought-prone site in Southern Siberia.

With the use of **quantitative wood anatomy** we could confirm that, within this environment, water availability was the factor most limiting growth during ring formation (e.g., Antonova and Stasova, 1993; Fonti and Babushkina, 2016). Despite the clear signature of SPEI on all the ring properties (both ring widths and tracheid size),

292 the timing and intensity of the water deficit constraining xylogenesis varied among the
293 analyzed traits (D_{EW}, D_{TW} and D_{LW}). Tracheid climatic signals were weaker than for the
294 ring width (RW) and with a dampening for the tracheids positioned later in the ring.
295 However, since their signal displayed a temporal delay, their composite signal well
296 covered most of the growing season (from May to July). These shifts in the climatic
297 signal are in accordance with previous xylogenesis studies on *P. sylvestris* growing in
298 forest-steppe (Antonova & Stasova, 1993; Antonova & Stasova, 2015). The relations
299 between tracheid size and water availability has been reported in a previous study
300 conducted in similar dry environments and explained as the results of water availability
301 constrains on the cell turgor pressure necessary for tracheid expansion (Eilmann et al.,
302 2011; Oberhuber et al., 2014). A similar mechanism can also explain the observed
303 positive effect of previous year November precipitation on tracheid size, which not only
304 provide a layer of snow that protect from frost damages during the winter (Babushkina
305 et al., 2015) but also represents an important source of additional water supply in the
306 following spring, when growth resumes. The release of signal strength observed when
307 comparing the two periods (early time 1964-1988 versus recent time 1989-2013)
308 support the control of water availability on growth, but it particularly also evidences the
309 importance of occurring changes in seasonality (specifically in amount of summer
310 precipitation) for *Pinus sylvestris* growth in such a dry environment. The climatic trends
311 observed over the 79 years period (1935-2013), quantifiable as a significant increase
312 (slope significantly different from 0, t-test, $P<0.05$) of 33.15 mm in the last two decades
313 (+ 9.6 % in total), represented an ideal opportunity to investigate the sensitivity of the
314 VS-model to capture the intra-annual change in tree growth.
315 Indeed, the **VS-model simulations** confirmed the important role of water availability on
316 daily tree growth, with water availability being the most limiting growth factor from

~115 DOY to ~228 DOY, i.e., for ~77% of the growing season length of the average (1940-2013) climatic year. The model simulations also displayed a growth limitation induced by temperature for the beginning and the end of the growing season. It thus confirms that late spring and early summer temperatures are critical for the onset of tree growth (Vaganov et al., 1999) since warm is provided for both the onset of cambial activity and snow melting (Kirdyanov et al., 2003).

The **combination of the approaches** (Quantitative wood anatomy and VS-modeling) applied to a gradient of aridity revealed valuable insights into the effect of changing seasonality on both the phenology and intra-annual rate of growth that matched with observations. In this context, many studies have already established that onset of cambial activity requires a minimal air temperature (Vaganov *et al.*, 1999; Rossi *et al.*, 2008), and that enough soil moisture is required to maintain the process active (Kramer, 1964). It would be therefore expected that temperature prior to xylogenesis (February) may promote an earlier onset of growth and larger growth rings, while a reduction in summer precipitation and increased temperature (late June and July) may lead to a increase in transpiration (Babushkina et al., 2015) and a reduced turgor pressure that eventually induces the formation of smaller and thicker latewood-like cells. The tree-growth simulation among the years grouped by aridity level revealed that the temperature limitation at the beginning and the end of the growing season only slightly modified the timing and amount of growth. This low impact is confirmed by the absence of positive temperature signal in late spring. In contrast, the control of water availability on modeled growth became evident when comparing the level of the intra-annual growth rates among the aridity groups (Dry, Medium and Wet). The release of summer drought mainly fostered the transition wood and latewood zones by increasing their widths by 28 and 48%, respectively. These results are coinciding with positive

342 growth response to May-June precipitation previously observed on *P. sylvestris*
343 (Babushkina et al., 2015; Shah et al., 2015) as well with measurements performed on
344 the collected cores, with an observed latewood growth increase from Dry to Wet years
345 of 41% in comparison with 21 % of increase in the earlywood. The responses are thus
346 revealing the important constraint of summer drought particularly on the second part of
347 the growth ring, which are consistent with previous findings by Eilmann et al. (2010,
348 2011) performed for the same species on an irrigation experimental site in a dry inner
349 alpine valley in Switzerland. Indeed, it is known that drought induces stomata closure in
350 *P. sylvestris* (Irvine et al., 1998; Martínez-Vilalta et al., 2009), thus consequently
351 reduces photosynthetic rates, carbon supply, and growth (McDowell, 2011; Olano *et al.*,
352 2014).
353 Since conifer tree-rings are characterized by two distinguished sectors (earlywood and
354 latewood) providing different primary functions, i.e., water transport in the earlywood
355 and mechanical stability in the latewood (Hacke et al., 2001), this differentiated impact
356 of climatic seasonality on LW over EW production may have significant unbalanced
357 consequences on the xylem functioning that need to be assessed. Our results showed
358 that water availability affected the size of earlywood tracheids but less their numbers,
359 while it strongly affected the amount of carbon rich latewood cells. Considering that
360 latewood cells require a large amount of carbon, the current seasonal increase in
361 summer precipitation is undoubtedly an indication of an increased carbon sink capacity
362 of *Pinus sylvestris* in southern Siberia. However, this positive trend might be newly
363 mitigated if the annual temperature increment expected in Russia (Anisimov et al.,
364 2008) will be confirmed.
365
366 **Conclusions**

The combination of quantitative wood anatomy and tree growth modeling has proved to be a valuable approach to provide higher-resolved insights of tree-ring intra-annual growth responses. Our assessment of the climatic impact on the different intra-ring sector widths via the VS-model based but using the timing of climatic sensitivity obtained from quantitative wood anatomy provided results well matching the observations. Such approach might thus be applied to assess impacts on tree-ring properties under different climate scenarios.

Specifically, in this study we could establish that the growth of *P. sylvestris* trees from a drought-prone site in Southern Siberia are currently profiting from an increased trend of summer precipitations. This positive effect becomes apparent as a generalized increased tracheid size (favoring water conduction) and especially as a majored width of the more carbon-demanding tree-ring sectors (+ 28.1– 48.6 % of transition and latewood), thus promoting a more mechanically stable wood structure that fixes a considerably higher amount of atmospheric carbon. The observed impacts that changes in seasonality had on the different intra-ring sectors are of high relevance considering the primary role (hydraulic and support) these sectors play for the functioning and survival of trees and their derived forest ecosystem services.

Acknowledgments

We are indebted with A. Kirdyanov for providing sampling and tree-ring measurements collected in the frame of the project [RSF 14-14-00295] and T. Kostyakova for the preparation of the cross-sections. A. Arzac contract was supported by the Russian Ministry of Education, Post-Doctoral Program of Project “5-100” [Grant № M 2.2.3] and by the Russian Science Foundation [Grant 14-14-00219-P, simulation modeling]. I. Sviderskaya has been supported by the Russian Science Foundation [15-14-30011]. E.

392 Babushkina and E.Vaganov were funded by Russian Foundation for Basic Research,
393 Government of Krasnoyarsk Territory, Krasnoyarsk Region Science and Technology
394 Support Fund to the research project # 17-44-240809/17
395

396 **References**

397 1. Agroclimatic Resources of Krasnoyarsk Krai and Tuva, 1974. ASSR, Leningrad.
398 2. Anchukaitis, K.J., Evans, M.N., Kaplan, A., Vaganov, E.A., Hughes, M.K.,
399 Grissino-Mayer, H.D., Cane, M.A., 2006. Forward modeling of regional scale tree-
400 ring patterns in the southeastern United States and the recent influence of summer
401 drought. Geophys. Res. Lett. 33, 2–5. doi:10.1029/2005GL025050
402 3. Anderegg, W.R.L., Flint, A., Huang, C., Flint, L., Berry, J.A., Davis, F.W., Sperry,
403 J.S., Field, C.B., 2015. Tree mortality predicted from drought-induced vascular
404 damage. Nat. Geosci. 8, 367–371. doi:10.1038/ngeo2400
405 4. Anisimov, O., Anokhin, Y., Boltneva, L., Vaganov, E.A., Gruza, G., Zaitsev, A.,
406 Zolotokrylin, A., Izrael, Y., Insarov, G., Karol, I., Kattsov, V., Kobysheva, N.,
407 Kostianoy, A., Krenke, A., Mescherskaya, A., Mirvis, V., Oganesyan, V., Pchelkin,
408 A., Revich, B., Reshetnikov, A., Semenov, V., Sirotenko, O., Sporyshev, P.,
409 Terziev, F., Frolov, I., Khon, V., Tsyban, A., Sherstyukov, B., Shiklomanov, I.,
410 YasukAnisimov, V., 2008. Assessment report on climate change and its
411 consequences in Russian Federation. General Summary. Federal Service for
412 Hydrometeorology and Environmental Monitoring (Roshydroment), Moscow, p.
413 24.
414 5. Antonova, G.F., Stasova, V. V., 1993. Effects of environmental factors on wood
415 formation in Scots pine stems. Trees 7, 214–219. doi:10.1007/BF00202076

6. Antonova, G.F., Stasova, V. V, 2015. Seasonal Distribution of Processes Responsible for Radial Diameter and Wall Thickness of Scots Pine Tracheids. Сибирский Лесной Журнал (Siberian Forest Journal) 33–40. doi:10.15372/SJFS20150203
7. Babushkina, E.A., Vaganov, E.A., Belokopytova, L. V, Shishov, V. V, Grachev, A.M., 2015. Competitive strength effect in the climate response of scots pine radial growth in south-central siberia forest-steppe. Tree-Ring Res. 71, 106–117. doi:10.3959/1536-1098-71.2.106
8. Beck, W., Sanders, TGM ., Pofahl, U. 2013. CLIMTREG: Detecting temporal changes in climate–growth reactions – A computer program using intra-annual daily and yearly moving time intervals of variable width. Dendrochronologia 31, 232–241. doi: 10.1016/j.dendro.2013.02.003
9. Björklund, J., Seftigen, K., Schweingruber, F., Fonti, P., von Arx, G., Bryukhanova, M. V., Cuny, H.E., Carrer, M., Castagneri, D., Frank, D.C., 2017. Cell size and wall dimensions drive distinct variability of earlywood and latewood density in Northern Hemisphere conifers. New Phytol. 216, 728–740. doi:10.1111/nph.14639
10. Camarero, J.J., Olano, J.M., Parras, A., 2010. Plastic bimodal xylogenesis in conifers from continental Mediterranean climates. New Phytol. 185, 471–480. doi:10.1111/j.1469-8137.2009.03073.x
11. Carrer, M., Castagneri, D., Prendin, A.L., Petit, G., von Arx, G., 2017. Retrospective Analysis of Wood Anatomical Traits Reveals a Recent Extension in Tree Cambial Activity in Two High-Elevation Conifers. Front. Plant Sci. 8, 1–13. doi:10.3389/fpls.2017.00737

12. Castagneri, D., Fonti, P., von Arx, G., Carrer, M., 2017. How does climate influence xylem morphogenesis over the growing season? Insights from long-term intra-ring anatomy in *Picea abies*. Ann. Bot. 119, 1011–1020. doi:10.1093/aob/mcw274
13. Cocozza, C., Palombo, C., Tognetti, R., Porta, N. La, Anichini, M., Giovannelli, A., Emiliani, G., 2016. Monitoring intra-annual dynamics of wood formation with microcores and dendrometers in *Picea abies* at two different altitudes. Tree Physiol. 36, 832–846. doi:10.1093/treephys/tpw009
14. Cook, E.R., Holmes, R., 1996. Guide for computer program ARSTAN. in: Grissino-Mayer, H.D., Holmes, R.L., Fritts, H.C. (Eds.), The International Tree-Ring Data Bank Program Library Version 2.0 User's Manual. Laboratory of Tree-Ring Research, University of Arizona, Tucson, USA, pp. 75–87.
15. Cook, E.R., Peters, K., 1981. The smoothing spline: a new approach to standardizing forest interior tree-ring width series for dendroclimatic studies. Tree-ring Bull. 41, 45–53.
16. Cuny, H.E., Rathgeber, C.B.K., Frank, D., Fonti, P., Fournier, M., 2014. Kinetics of tracheid development explain conifer tree-ring structure. New Phytol. 203, 1231–1241. doi:10.1111/nph.12871
17. Dengler, N.G., 2001. Regulation of vascular development. J. Plant Growth Regul. 20, 1–13. doi:10.1007/s003440010008
18. Dixon, R.K., Brown, S., Houghton, R., Solomon, A., Trexler, M., Wisniewski, J., 1994. Carbon Pools and Flux of Global Forest Ecosystems. Science. 263, 185–190. doi: 10.1126/science.263.5144.185.
19. Eckstein, D., 2004. Change in past environments–secrets of the tree hydrosystem. New Phytol. 163, 1–4. doi: 10.1111/j.1469-8137.2004.01117.x

20. Eilmann, B., Buchmann, N., Siegwolf, R., Saurer, M., Cherubini, P., Rigling, A., 2010. Fast response of Scots pine to improved water availability reflected in tree-ring width and delta 13C. Plant Cell Environ. 33, 1351–60. doi:10.1111/j.1365-3040.2010.02153.x

21. Eilmann, B., Zweifel, R., Buchmann, N., Graf Pannatier, E., Rigling, A., 2011. Drought alters timing, quantity, and quality of wood formation in Scots pine. J. Exp. Bot. 62, 2763–2771. doi:10.1093/jxb/erq443

22. Evans, M.N., Reichert, B.K., Kaplan, A., Anchukaitis, K.J., Vaganov, E.A., Hughes, M.K., Cane, M.A., 2006. A forward modeling approach to paleoclimatic interpretation of tree-ring data. J. Geophys. Res. Biogeosciences 111, 1–13. doi:10.1029/2006JG000166

23. Fonti, P., Babushkina, E.A., 2016. Tracheid anatomical responses to climate in a forest-steppe in Southern Siberia. Dendrochronologia 39, 32–41. doi:10.1016/j.dendro.2015.09.002

24. Fonti, P., Jansen, S., 2012. Xylem plasticity in response to climate. New Phytol. 195, 734–736. doi:10.1111/j.1469-8137.2012.04252.x

25. Fonti, P., Von Arx, G., García-González, I., Eilmann, B., Sass-Klassen, U., Gärtner, H., Eckstein, D., 2010. Studying global change through investigation of the plastic responses of xylem anatomy in tree rings. New Phytol. 185, 42–53. doi: 10.1111/j.1469-8137.2009.03030.x

26. Frank, D., Reichstein, M., Bahn, M., Thonicke, K., Frank, D., Mahecha, M.D., Smith, P., van der Velde, M., Vicca, S., Babst, F., Beer, C., Buchmann, N., Canadell, J.G., Ciais, P., Cramer, W., Ibrom, A., Miglietta, F., Poulter, B., Rammig, A., Seneviratne, S.I., Walz, A., Wattenbach, M., Zavala, M.A., Zscheischler, J., 2015. Effects of climate extremes on the terrestrial carbon cycle: Concepts,

processes and potential future impacts. Glob. Chang. Biol. 21, 2861–2880. doi:10.1111/gcb.12916

27. Grissino-Mayer, H.D., 2001. Evaluating crossdating accuracy: a manual and tutorial for the computer program COFECHA. Tree-Ring Res. 57, 205–221.

28. Hacke, U., Sperry, J.J.S., Pockman, W.T.W., Davis, S.D.S., McCulloh, K.A., 2001. Trends in wood density and structure are linked to prevention of xylem implosion by negative pressure. Oecologia 126, 457–461. doi:10.1007/s004420100628

29. Hereş, A.M., Camarero, J.J., López, B.C., Martínez-Vilalta, J., 2014. Declining hydraulic performances and low carbon investments in tree rings predate Scots pine drought-induced mortality. Trees - Struct. Funct. 28, 1737–1750. doi:10.1007/s00468-014-1081-3

30. Hsiao, T.C., Acevedo, E., 1974. Plant responses to water deficits, water-use efficiency, and drought resistance. Agric. Meteorol. 14, 59–84. doi:10.1016/0002-1571(74)90011-9

31. Irvine, J., Perks, M.P., Magnani, F., Grace, J., 1998. The response of *Pinus sylvestris* to drought: stomatal control of transpiration and hydraulic conductance. Tree Physiol. 18, 393–402. doi:10.1093/treephys/18.6.393

32. Kirdyanov, A., Hughes, M., Vaganov, E.A., Schweingruber, F., Silkin, P., 2003. The importance of early summer temperature and date of snow melt for tree growth in the Siberian Subarctic. Trees 17, 61–69. doi: 10.1007/s00468-002-0209-z

33. Kramer, P., 1964. The role of water in wood formation, in: Zimmermann, M. (Ed.), The Formation of Wood in Forest Trees. Academic Press, New York, pp. 519–532.

34. Lal, R., 2008. Sequestration of atmospheric CO2 in global carbon pools. Energy Environ. Sci. 1, 86–100. doi:10.1039/b809492f

514 35. Martínez-Vilalta, J., Cochard, H., Mencuccini, M., Sterck, F., Herrero, A.,
515 Korhonen, J.F.J., Llorens, P., Nikinmaa, E., Nolè, A., Poyatos, R., Ripullone, F.,
516 Sass-Klaassen, U., Zweifel, R., 2009. Hydraulic adjustment of Scots pine across
517 Europe. New Phytol. 184, 353–364. doi:10.1111/j.1469-8137.2009.02954.x
518 36. McDowell, N.G., 2011. Mechanisms Linking Drought, Hydraulics, Carbon
519 Metabolism, and Vegetation Mortality. Plant Physiol. 155, 1051–9.
520 doi:10.1104/pp.110.170704
521 37. Nikolov, R., Helmisaari, N., 1992. Silvics of the circumpolar boreal forest tree
522 species, in: Shugart, H., Leeman, R., Bonan, G. (Eds.), A Systems Analysis of the
523 Globa Boreal Forest. CambridgeUniversityPress, New York, pp. 13–84.
524 38. Oberhuber, W., Gruber, A., Kofler, W., Swidrak, I., 2014. Radial stem growth in
525 response to microclimate and soil moisture in a drought-prone mixed coniferous
526 forest at an inner Alpine site. Eur. J. For. Res. 133, 467–479. doi:10.1007/s10342-
527 013-0777-z
528 39. Oladi, R., Elzami, E., Pourtahmasi, K., Bräuning, A., 2017. Weather factors
529 controlling growth of Oriental beech are on the turn over the growing season. Eur.
530 J. For. Res. 136, 345–356. doi: 10.1007/s10342-017-1036-5.
531 40. Olano, J.M., Eugenio, M., García-Cervigón, A.I., Folch, M., Rozas, V., 2012.
532 Quantitative Tracheid Anatomy Reveals a Complex Environmental Control of
533 Wood Structure in Continental Mediterranean Climate. Int. J. Plant Sci. 173, 137–
534 149. doi:10.1086/663165
535 41. Olano, J.M., Linares, J.C., García-Cervigón, A.I., Arzac, A., Delgado, A., Rozas,
536 V., 2014. Drought-induced increase in water-use efficiency reduces secondary tree
537 growth and tracheid wall thickness in a Mediterranean conifer. Oecologia 176,
538 273–283. doi:10.1007/s00442-014-2989-4

42. Rathgeber, C.B.K., 2017. Conifer tree-ring density inter-annual variability - anatomical, physiological and environmental determinants. New Phytol. 216, 621–625. doi:10.1111/nph.14763
43. Rathgeber, C.B.K., Cuny, H.E., Fonti, P., 2016. Biological Basis of Tree-Ring Formation: A Crash Course. Front. Plant Sci. 7, 1–7. doi:10.3389/fpls.2016.00734
44. Rossi, S., Deslauriers, A., Anfodillo, T., 2006. Assessment of cambial activity and xylogenesis by microsampling tree species: An example at the Alpine timberline. IAWA J. 27, 383–394. doi:10.1163/22941932-90000161
45. Rossi, S., Deslauriers, A., Gričar, J., Seo, J.-W., Rathgeber, C., Anfodillo, T., Morin, H., Levanic, T., Oven, P., Jalkanen, R., 2008. Critical temperatures for xylogenesis in conifers of cold climates. Glob. Ecol. Biogeogr. 17, 696–707. doi: 10.1111/j.1466-8238.2008.00417.x
46. Růžička, K., Ursache, R., Hejátko, J., Helariutta, Y., 2015. Xylem development - from the cradle to the grave. New Phytol. 207, 519–535. doi:10.1111/nph.13383
47. Sass-Klaassen, U., Fonti, P., Cherubini, P., Gričar, J., Robert, E.M.R., Steppe, K., Bräuning, A., 2016. A Tree-Centered Approach to Assess Impacts of Extreme Climatic Events on Forests. Front. Plant Sci. 7, 1–6. doi:10.3389/fpls.2016.01069
48. Schweingruber, F., Poschlod, P., 2005. Growth rings in herbs and shrubs: life span, age determination and stem anatomy. For. snow Landsc. Res. 79, 197–300.
49. Shah, S.K., Touchan, R., Babushkina, E., Shishov, V.V., Meko, D.M., Abramenko, O. V., Belokopytova, L. V., Hordo, M., Jevšenak, J., Kędziora, W., Kostyakova, T.V., Moskwa, A., Oleksiak, Z., Omurova, G., Ovchinnikov, S., Sadeghpour, M., Saikia, A., Zsewastynowicz, Ł., Sidenko, T., Strantsov, A., Tamkevičiūtė, M., Tomusiak, R., Tychkov, I., 2015. August to July Precipitation from Tree Rings in

563 the Forest-Steppe Zone of Central Siberia (Russia). Tree-Ring Res. 71, 37–44.
564 doi:10.3959/1536-1098-71.1.37
565 50. Shishov, V.V., Tychkov, I.I., Popkova, M.I., Ilyin, V.A., Bryukhanova, M. V.,
566 Kirdyanov, A. V., 2016. VS-oscilloscope: A new tool to parameterize tree radial
567 growth based on climate conditions. Dendrochronologia 39, 42–50.
568 doi:10.1016/j.dendro.2015.10.001
569 51. Silkin, P.P., 2010. Methods of Multiparameter Analysis of Conifers Tree-rings
570 Structure. Siberian Federal University, Krasnoyarsk.
571 52. Steppe, K., Sterck, F., Deslauriers, A., 2015. Diel growth dynamics in tree stems:
572 linking anatomy and ecophysiology. Trends Plant Sci. 20, 335–343.
573 doi:10.1016/j.tplants.2015.03.015
574 53. Vaganov, E.A., 1990. The Tracheidogram Method in Tree-Ring Analysis and Its
575 Application, in: Cook, E., Kairiukstis, L. (Eds.), Methods of Dendrochronology.
576 Springer Netherlands, pp. 63–76. doi:10.1007/978-94-015-7879-0
577 54. Vaganov, E.A., Hughes, M.K., Shashkin, A.V, 2006. Growth Dynamics of Conifer
578 Tree Rings Images of Past and Future Environments. Springer-Verlag Berlin
579 Heidelberg. doi:10.1017/CBO9781107415324.004
580 55. Vaganov, E.A., Hughes, M.K., Kirdyanov, A.V, Schweingruber, F.H., Silkin, P.P.,
581 1999. Influence of snowfall and melt timing on tree growth in subarctic Eurasia.
582 Nature 400, 149–151. doi:10.1038/22087
583 56. Vicente-Serrano, S.M., Beguería, S., López-Moreno, J.I., 2010. A multi-scalar
584 drought index sensitive to global warming: the Standardized Precipitation
585 Evapotranspiration Index–SPEI. J. Clim. 23, 1696–1718. doi:
586 10.1175/2009JCLI2909.1

57. Zhao, M., Running, S.W., 2010. Drought-Induced Reduction in Global Terrestrial Net Primary Production from 2000 Through 2009. Science. 329, 940–943. doi:10.1126/science.1192666

592 **Tables and figures**

593 **Table 1.** Overview of the tree-ring traits analyzed in this work

Anatomical trait	Acronym	Unit
Tree-ring width	RW	µm
Lumen radial diameter	LRD	µm
Cell wall thickness	CWT	µm
Tracheid radial diameter	D	µm
Maximum cell radial diameter in the earlywood	D_{EW}	µm
Maximum cell radial diameter in the transition wood	D_{TW}	µm
Radial diameter of the latewood cell with maximum wall thickness	D_{LW}	µm

594

Table 2. Pearson's correlations between the tree-ring chronologies and the mean monthly climatic parameters (P = precipitation; T = temperature; SPEI index with a 1 month time-scale) for the period 1964 – 2013. Uppercase letters refers to previous year and lowercase letters to current year. T and P data are from the meteorological station of Minusinsk (53°70'N, 91°70'E), SPEI data is available at http://spei.csic.es/database.html.

		SEP	OCT	NOV	DEC	jan	feb	mar	apr	may	jun	jul	aug	sep
P	RW	*0.26*	0.17	**0.56**	0.02	*0.26*	*0.31*	-0.06	0.11	**0.62**	0.23	*0.25*	-0.14	*-0.25*
	D_{EW}	0.17	-0.03	**0.44**	0.12	0.08	0.05	0.00	0.18	**0.45**	*0.25*	0.18	-0.19	-0.02
	D_{TW}	*0.30*	-0.07	*0.29*	*0.26*	-0.03	0.00	0.02	0.02	-0.02	**0.51**	*0.29*	-0.17	0.13
	D_{LW}	0.10	0.19	**0.44**	0.01	0.07	**0.46**	-0.02	0.35	*0.30*	0.13	**0.51**	0.01	-0.07
T	RW	-0.23	-0.03	-0.15	-0.18	0.07	0.18	-0.14	0.06	*-0.32*	-0.21	-0.36	*-0.27*	0.07
	D_{EW}	*-0.27*	0.01	-0.20	-0.07	0.09	*0.25*	0.03	0.04	-0.16	-0.42	*-0.24*	-0.08	-0.10
	D_{TW}	-0.06	0.06	0.05	-0.16	-0.08	0.17	-0.03	-0.03	-0.07	-0.17	-0.39	-0.15	-0.14
	D_{LW}	-0.05	0.03	-0.05	-0.20	0.18	0.00	-0.18	-0.04	*-0.26*	-0.13	**-0.44**	*-0.25*	-0.18
SPEI (1 month)	RW	-0.22	-0.05	-0.13	-0.18	0.22	0.21	0.03	0.03	**0.54**	*0.28*	*0.25*	-0.08	*-0.24*
	D_{EW}	0.07	-0.11	-0.11	-0.16	0.08	0.10	0.00	0.10	0.38	0.34	0.14	-0.09	0.05
	D_{TW}	0.09	-0.04	-0.11	-0.08	-0.08	-0.07	-0.05	-0.08	-0.04	**0.59**	0.33	-0.16	0.11
	D_{LW}	-0.03	-0.05	-0.22	-0.07	0.06	*0.26*	-0.01	0.21	0.22	0.23	**0.54**	-0.08	-0.02

Coefficients in bold are significant at $P < 0.001$, underlined coefficients are significant at $P < 0.01$ and coefficients in italic are significant at $P < 0.05$.

Table 3. Pearson's correlations between the tree-ring chronologies and the mean monthly climatic parameters (P = precipitation; T = temperature; SPEI index with a 1-month time-scale) separated into two periods (early time 1964-1988, and recent time 1989-2013). Correlations only include the current year growing season, i.e. the months from May to August.

		1964-1988				1989-2013			
		may	jun	jul	aug	may	jun	jul	aug
P	RW	**0.75**	0.27	0.34	0.14	**0.52**	0.22	0.10	-0.40
	D_{EW}	**0.51**	0.24	0.36	-	***0.45***	0.25	-0.20	-
	D_{TW}	0.12	0.35	0.33	0.32	-0.08	**0.59**	0.26	**-0.58**
	D_{LW}	**0.58**	0.12	**0.51**	0.01	0.06	0.38	-0.31	-0.21
T	RW	-0.44	-0.12	-0.36	-0.29	-0.26	-0.30	-0.38	-0.26
	D_{EW}	**-0.51**	-0.39	-0.27	-	0.15	**-0.46**	-0.22	-
	D_{TW}	-0.30	-0.41	**-0.50**	-0.29	-0.04	-0.01	-0.43	-0.13
	D_{LW}	-0.45	-0.20	**-0.47**	-0.20	-0.39	**-0.47**	0.22	0.36
SPEI	RW	**0.73**	0.32	0.42	0.11	0.40	0.27	0.05	-0.26
	D_{EW}	**0.52**	0.30	0.40	-	0.27	0.41	-0.23	-
	D_{TW}	0.16	0.38	0.33	0.36	-0.12	0.74	0.33	**-0.57**
	D_{LW}	**0.57**	0.18	**0.56**	-0.04	-0.06	0.31	**0.53**	-0.10

Highly significant correlations ($P < 0.01$) are bold; significant correlations ($P < 0.05$) are underlined.

Table 4. Cumulative growth rates as obtained from the calibrated VS-model (Table S.2) using the DOYs showing a significant ($P < 0.05$) climate signal (see Fig. 3) and from the measured EW and LW widths grouped by aridity level (Dry, Medium and Wet). The % increase indicates the increase of cumulated growth of the Wet group relative to the Dry one. D_{EW} = maximum cell radial diameter in the earlywood; D_{TW} = maximum cell radial diameter in the transition wood; D_{LW} = radial diameter of the latewood cell with maximum radial wall thickness; Rest = period of the growing season (Fig. 4) which is not covered by the climatic signal of D_{EW}, D_{TW} and D_{LW}.

		From the model				From measurements	
		D_{EW}	D_{TW}	D_{LW}	Rest	EW+TW (µm)	LW (µm)
Aridity	Dry	16.71	14.74	6.79	12.53	949.64	220.28
	Medium	15.26	15.76	8.23	13.75	1095.05	260.16
	Wet	18.13	18.89	10.09	17.59	1154.02	311.27
	% increase	8.50	28.15	48.60	40.38	21.52	41.31

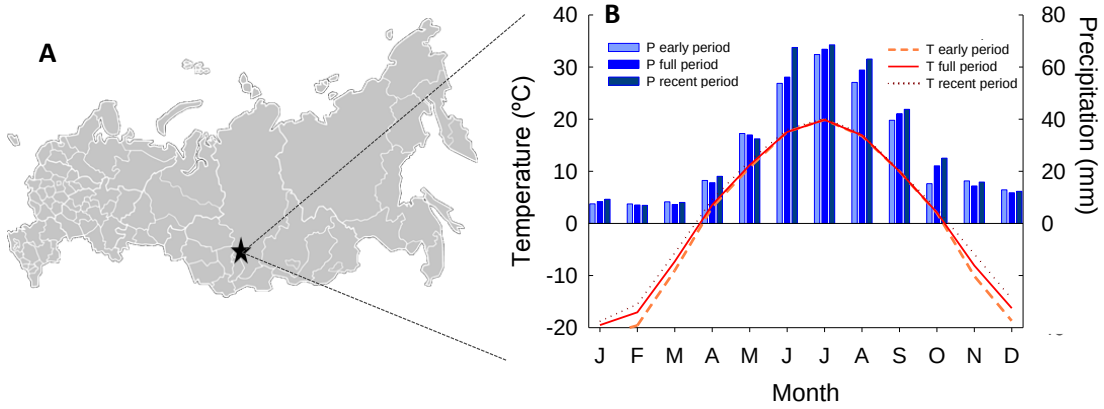

627

628 **Figure 1.** Site location and climate. (A) Location of the study site (black star) within the

629 map of the Russian Federation and, (B) climatic diagram for the nearby located climate

630 station of Minusinsk. The diagram shows the monthly averages for the full data

631 coverage (1935-2013, n=79) and separated for the early (1935-1954, n=20) and recent

632 (1994-2013, n=20) period. Bars show monthly precipitation and lines monthly mean

633 temperature.

634

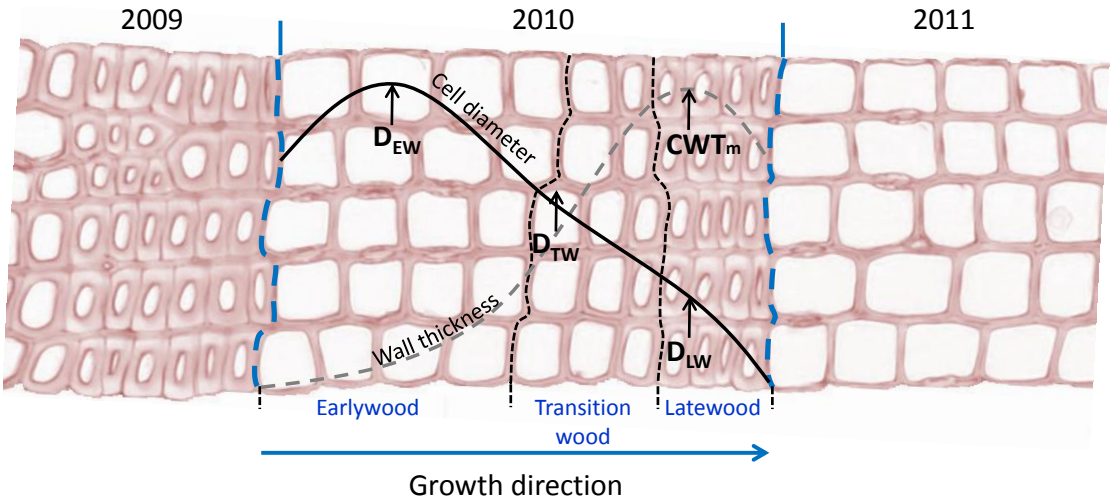

635

636 **Figure 2.** Schema of a *Pinus sylvestris* xylem cross-section indicating the determination

637 of the parameters D_{EW}, D_{TW}, D_{LW} and CWT_m. Solid line shows the tracheidogram of the

638 cell diameter. Dashed line shows the tracheidogram of the cell wall thickness. Vertical

639 dashed blue lines border the 2010 tree ring; dashed black lines delimit the earlywood,

640 transition wood, and latewood zones within the 2010 annual ring. Transition wood was

641 defined considering the development of the tracheid diameter and wall thickness along

642 the annual ring radial direction. The transition wood initiates when the wall thickness

643 gets larger than the tracheid lumen diameter and it ends when cell wall thickness start to

644 level off (at CWT_m position).

645

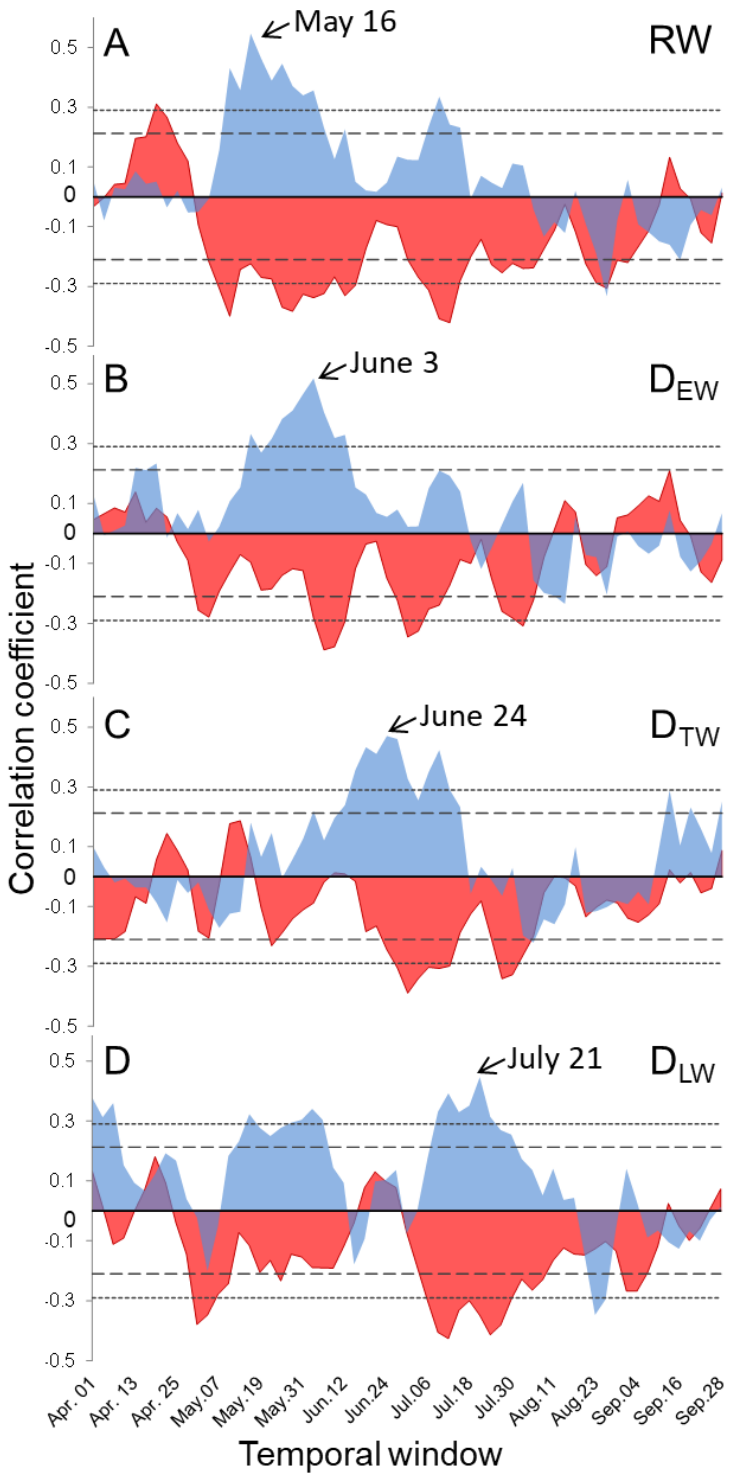

Figure 3. Moving correlations (11-days window) between tree-ring width (RW) and tracheid diameter in the earlywood (D_{EW}), transition wood (D_{TW}) and latewood (D_{LW}) with the April-September temperature and precipitation over the period 1964-2013. Blue color represents precipitation and red is for temperature. Lines indicate significant correlation threshold for (dashed line at $P < 0.05$ and dotted line for $P < 0.01$; n = 50).

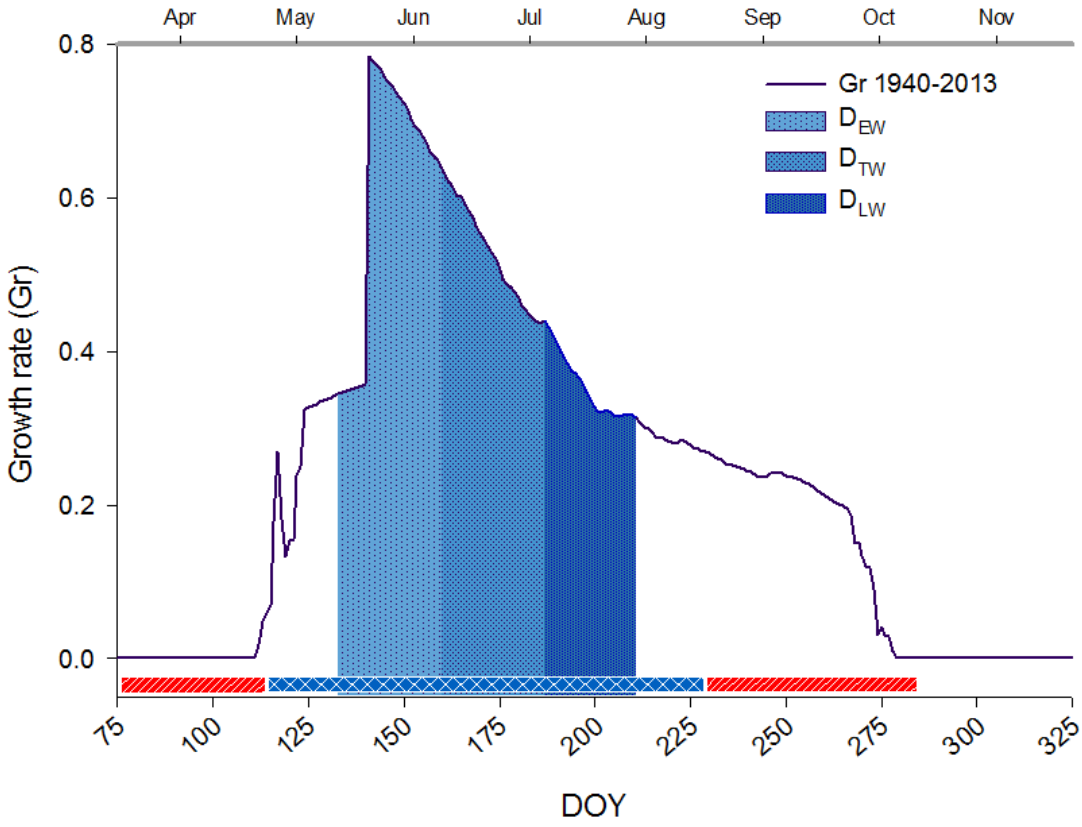

652

653 **Figure 4.** Daily growth rates generated by the VS-model considering the average
654 climatic data over the period 1940-2013. Horizontal colored bars indicate periods in
655 which temperature (red) or soil moisture (blue) most limit growth. Vertical segments
656 represent the period in which the anatomical traits correlate significantly (P<0.05) with
657 the precipitation, i.e.; between DOY 133-163, DOY 160-196 and DOY 187-194 for
658 $D_{EW,}$ $D_{TW,}$ and D_{LW}, respectively (Fig. 3).

659

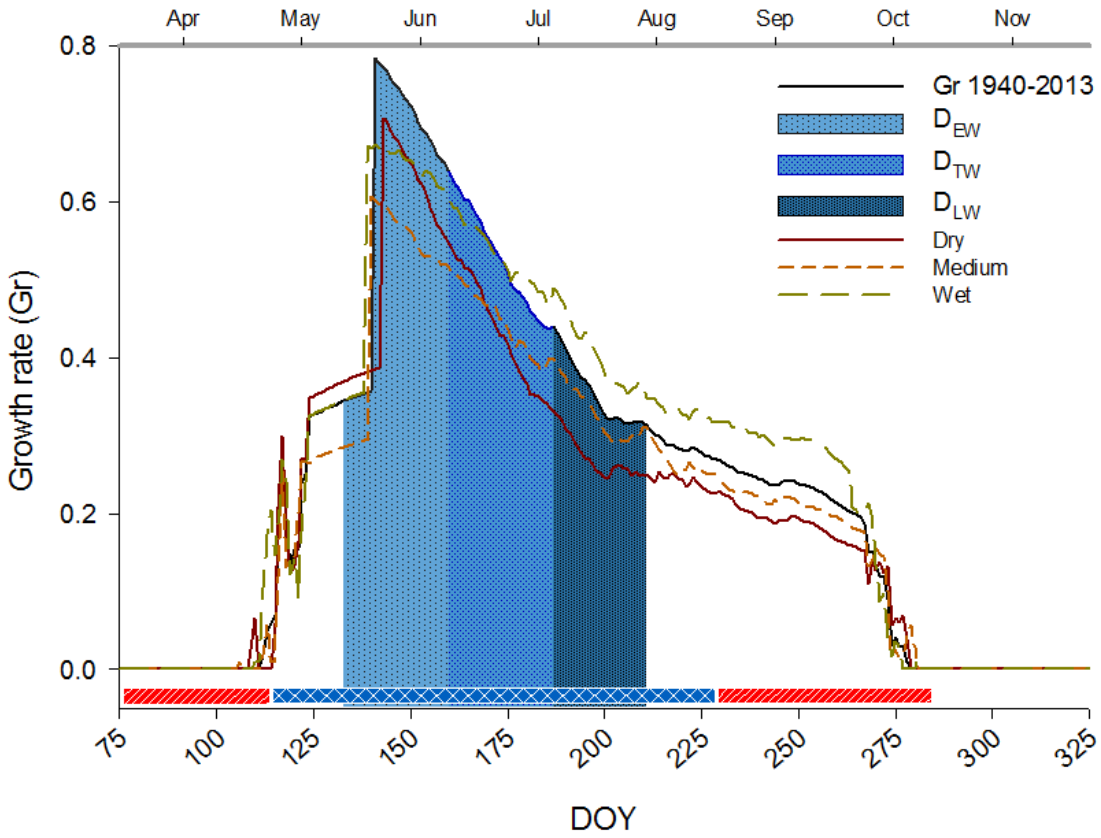

660

661 **Figure 5.** Daily growth rates generated by the VS-model considering the average
662 climatic data of the years grouped by growing season aridity index (i.e., Dry, Medium
663 and Wet, Table 4). Horizontal colored bars indicate periods in which temperature (red)
664 or soil moisture (blue) most limit growth. Vertical segments represent period in which
665 the anatomical traits correlate significantly (P<0.05) with precipitation (Fig. 3), i.e.;
666 between DOY 133-163, DOY 160-196 and DOY 187-194 for D_{EW}, D_{TW}, and D_{LW},
667 respectively.

668

669

Supplementary materials

Table S.1. Pairwise Pearson's correlations among the standardized chronologies.

	RW	D_{EW}	D_{TW}	D_{LW}	CWT_m
N	**0.96**	**0.55**	*0.25*	**0.63**	**0.65**
RW		**0.67**	0.40	**0.67**	**0.64**
D_{EW}	**0.67**		**0.53**	**0.48**	**0.53**
D_{TW}	0.40	**0.53**		0.40	*0.33*
D_{LW}	**0.67**	**0.48**	0.40		**0.68**

Coefficients in bold are significant at $P < 0.001$, underlined coefficients are significant at $P < 0.01$ and coefficients in italic are significant at $P < 0.05$. N = number of cells along the tracheidogram; RW = tree-ring width; D_{EW} = maximum cell radial diameter in the earlywood; D_{TW} = maximum cell radial diameter in the transition wood; D_{LW} = radial diameter of the latewood cell with maximum radial wall thickness; CWT_m = maximum cell wall thickness

Table S.2. Calibrated VS-model.

Parameter	Description	Value
T_{min}	Minimum temperature for tree growth (^oC)	5
T_{opt1}	Lower end of range of optimal temperatures (^oC)	13
T_{opt2}	Upper end of range of optimal temperatures (^oC)	22
T_{max}	Maximum temperature for tree growth (^oC)	32
W_{min}	Minimum soil moisture for tree growth, relative to saturated soil (v/vs)	0.0775
W_{opt1}	Lower end of range of optimal soil moistures (v/vs)	0.25
W_{opt2}	Upper end of range of optimal soil moistures (v/vs)	0.375
W_{max}	Maximum soil moisture for tree growth (v/vs)	0.45
W_0	Initial soil moisture (v/vs)	0.15
T_{beg}	Temperature sum for initiation of growth (^oC)	110
t_{beg}	Time period for temperature sum (days)	10
l_r	Depth of root system (mm)	500
P_{max}	Maximum daily precipitation for saturated soil (mm/day)	40
C_1	Fraction of precip. penetrating soil (not caught by crown) (rel. unit)	0.5
C_2	First coefficient for calculation of transpiration (mm/day)	0.3075
C_3	Second coefficient for calculation of transpiration (mm/day)	0.11
Λ	Coefficient for water drainage from soil (rel. unit)	0.005
V_{cr}	Critical growth rate	0.04

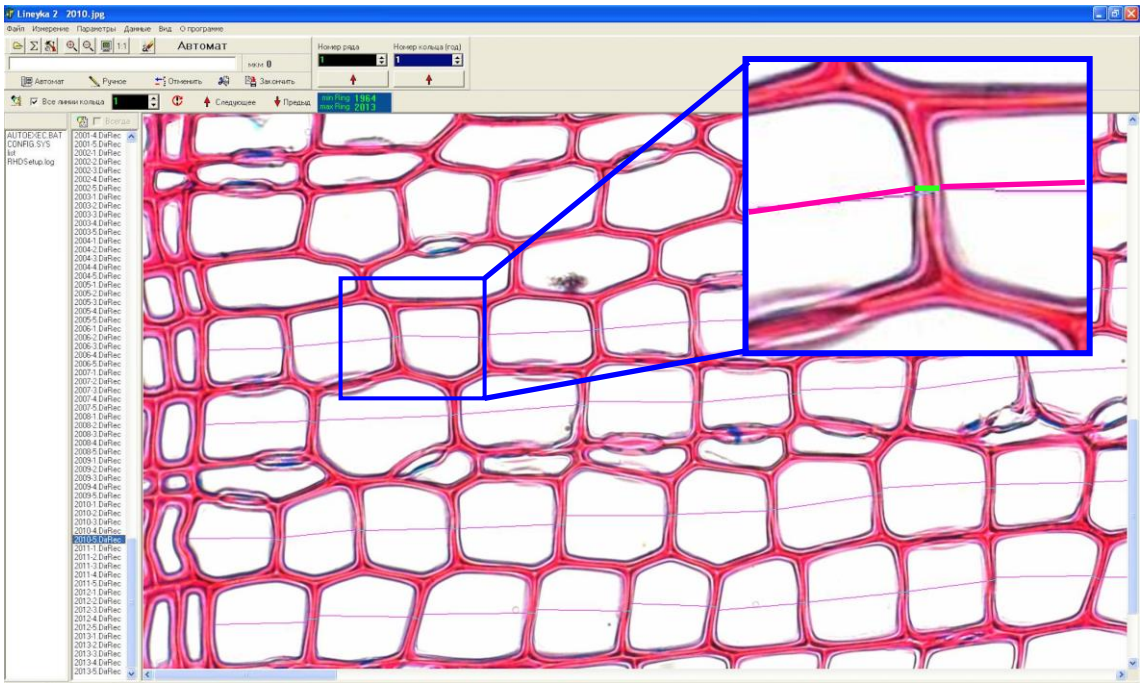

Figure S.1. Lineyka print screen showing how the measurements have been performed for the tracheid along selected radial files. Pink segments indicate the measurement of the radial lumen diameter; green segments indicate the measurement of the double cell wall thickness along the radial direction of the tracheid tangential wall.

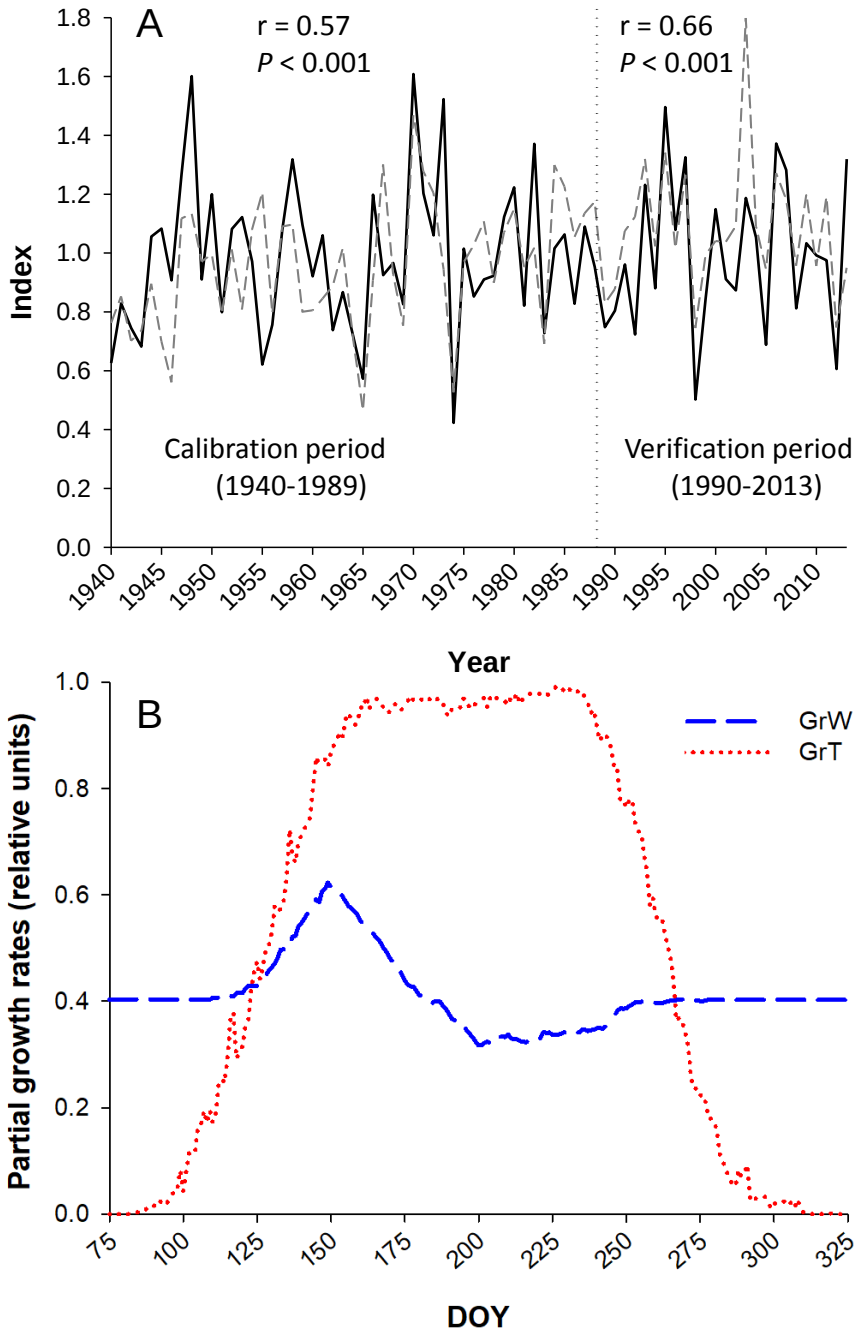

690

691 **Figure S.2.** (A) Comparison between original (solid line) and VS-model (dashed line)
692 tree-ring chronologies. The VS-oscilloscope has been used to parameterize the model
693 (Table S2). Correlation (r) and level of significance (p) are given for both the calibration
694 (1940-1989) and verification (1990-2013) periods. (B) Daily growth rates as limited by
695 temperature (dotted line) and soil moisture (dashed line).

696